

$W^\pm + 4\text{jet}$ irreducible background events from QCD in top and Higgs searches at the Next Linear Collider

Stefano Moretti

*Cavendish Laboratory, University of Cambridge,
Madingley Road, Cambridge CB3 0HE, UK.*

Abstract

Irreducible background effects due to $e^+e^- \rightarrow W^\pm + bbjj$ and $e^+e^- \rightarrow W^\pm + jjjj$ events produced via QCD in top-antitop production and heavy Higgs searches in the bremsstrahlung channel are studied at the Next Linear Collider. Various distributions relevant to phenomenological analyses are given and compared to those expected from top and Higgs signals in the decay channel $b\bar{b}W^+W^- \rightarrow b\bar{b}W^\pm jj$. This analysis follows similar ones previously carried out for the case of the irreducible background proceeding via electroweak interactions.

1. Introduction

In a series of recent papers [1, 2, 3] various effects due to the irreducible background in $e^+e^- \rightarrow b\bar{b}W^+W^-$ (with $W^+W^- \rightarrow W^\pm + jj$) electroweak (EW) events in top and Higgs searches at the Next Linear Collider (NLC) were calculated, both within the Standard Model (\mathcal{SM}) [1, 3] and the Minimal Supersymmetric Standard Model (\mathcal{MSSM}) [2]. On the one hand, top quarks are produced in pairs in electron-positron annihilations, through the mechanism $e^+e^- \rightarrow \gamma^*, Z^* \rightarrow t\bar{t}$, and they subsequently decay via $t \rightarrow bW^\pm$ (if Supersymmetry is present also into, e.g., $t \rightarrow bH^\pm$, via charged Higgses). On the other hand, Higgs signatures¹ giving $b\bar{b}W^+W^-$ final states are those produced in the processes $e^+e^- \rightarrow Z\phi$ (for the \mathcal{SM} , see Ref. [1]) and $e^+e^- \rightarrow ZH$, $e^+e^- \rightarrow AH$, $e^+e^- \rightarrow hW^+W^-$ (for the \mathcal{MSSM} , see Ref. [2]), in which Z , A and h decay into $b\bar{b}$ pairs, and $\phi, H \rightarrow W^+W^-$.

The relevance of non-resonant $e^+e^- \rightarrow b\bar{b}W^+W^-$ EW diagrams, as well as their interplay with the signals, in the context of top and Higgs searches at the NLC ($\sqrt{s} = 350, 500$ GeV), has been demonstrated in the mentioned papers, to which we refer the reader for details. In general, irreducible background effects via EW interactions amount to several percents of the total $e^+e^- \rightarrow b\bar{b}W^+W^-$ cross section. They are particularly visible in the spectrum of the W^\pm momentum at the $t\bar{t}$ threshold, in the top-antitop excitation curve, as well as they can be relevant for some of the distributions in the $b\bar{b}$ and W^+W^- invariant masses. In all these cases, their knowledge is essential in order to perform at the NLC the foreseen high precision measurements of top and Higgs parameters [4].

It is the purpose of this short letter to calculate irreducible background effects to the mentioned signals due to QCD events yielding the signature $W^\pm + 4\text{jets}$ (in which the W^\pm can decay either hadronically or leptonically): that is, when the partons in the final state are produced through the order α_s^2 , via gluon (G) interactions. These can occur in

$$W^\pm + q\bar{q}'Q\bar{Q} \quad (\text{Fig. 1a}) \quad (1)$$

and

$$W^\pm + q\bar{q}'GG \quad (\text{Fig. 1b}) \quad (2)$$

partonic events. Since heavy flavour tagging (of b -quarks, essentially) will constitute one of the most powerful experimental tools in hadronic phenomenology at the NLC², the signature of the above mechanisms is actually made up by the following two components (b indicates both a b and a \bar{b}):

$$W^\pm + bbjj, \quad (3)$$

and

$$W^\pm + jjjj, \quad (4)$$

depending on the possible heavy (i.e., b) and light (i.e., j) quark content of processes (1)–(2). Their relative importance in the total sample of $W^\pm + 4\text{jets}$ is dictated by the partonic production rates as well as by the b -tagging efficiency/rejection that will be achieved by the NLC detectors.

¹In the following ϕ represents the \mathcal{SM} Higgs and h, H and A the \mathcal{MSSM} (neutral) counterparts.

²One should recall that the $b\bar{b}$ decay channel is largely dominant for Higgs bosons in the intermediate mass range, this rendering the detection of such particles rather problematic at the Large Hadron Collider (LHC) [5, 6], because of the QCD background, whereas the latter will not constitute a serious problem at the NLC.

Before exposing the plan of the paper, it is probably worth reminding the reader the importance of the $W^\pm + 4\text{jet}$ signature arising from $b\bar{b}W^+W^-$ production and decay. In fact, two leptonic W^\pm decays would lead to a double disadvantage: first, a very much reduced statistics and, second, problems in reconstructing invariant mass spectra because of the two neutrinos escaping detection. Thus, at least one of the W^\pm 's will most likely be tagged in the hadronic channel. Furthermore, between the two possible decays of the second W^\pm , it is usually preferred to resort to the leptonic final state (i.e., $W^\pm \rightarrow \ell\nu_\ell$, $\ell = e, \mu$), more than to the hadronic one (i.e., $W^\pm \rightarrow jj$). In fact, the experimental signature arising from the former has a few advantages with respect to the one from the latter: it has a simpler topology inside the detectors and thus it is easier to reconstruct; it also allows one to get rid of complications due to the combinatorics in case of a six jet final state; and finally, like the pure hadronic final state, its kinematics is fully constrained (once the missing momentum is assigned to the neutrino).

We proceed in the rest of the paper as follows: the next Section is devoted to a brief description of our computational method and to the declaration of the parameters used; the last one to a discussion of the results with a brief summary in the end.

2. Calculation

The computation of the matrix elements of the elementary processes $e^+e^- \rightarrow W^\pm + q\bar{q}'Q\bar{Q}$ (26 Feynman graphs) and $e^+e^- \rightarrow W^\pm + q\bar{q}'GG$ (84 Feynman graphs), with $q^{(\prime)}, Q = u, d, s, c$ and b , has been performed with the help of `MadGraph` [7], which uses the subroutines contained in `HELAS` [8], and the integrals over the phase spaces have been performed using the package `VEGAS` [9].

In the calculations we have adopted the following numerical values for the various parameters:

$$\begin{aligned}
m_e = m_u = m_d = 0, & \quad m_s = 0.3 \text{ GeV}, & \quad m_c = 1.4 \text{ GeV}, & \quad m_b = 4.25 \text{ GeV}, \\
M_Z = 91.175 \text{ GeV}, & \quad \Gamma_Z = 2.5 \text{ GeV}, \\
M_W = 80.23 \text{ GeV}, & \quad \Gamma_W = 2.08 \text{ GeV}, \\
G_F = 1.16637 \times 10^{-5} \text{ GeV}^{-2}, & \quad \alpha_{em} \equiv \alpha_{em}(M_Z) = 1/128.
\end{aligned} \tag{5}$$

Note that the charged and neutral weak fermion–boson couplings are defined by

$$g_W^2 = \frac{e^2}{\sin^2 \theta_W} = 4\sqrt{2}G_F M_W^2, \quad g_Z^2 = \frac{e^2}{\sin^2 \theta_W \cos^2 \theta_W} = 4\sqrt{2}G_F M_Z^2. \tag{6}$$

For the vector and axial couplings of the gauge bosons to the fermions, we use the ‘effective leptonic’ value

$$\sin^2(\theta_W) \equiv \sin_{eff}^2(\theta_W) = 0.2320. \tag{7}$$

The strong coupling constant α_s has been evaluated at two loops, with $N_f = 5$ and $\Lambda_{\overline{MS}} = 190 \text{ MeV}$, at the scale $Q^2 = s$, yielding $\alpha_s(M_Z^2) = 0.115$. Finally, the centre-of-mass (CM) energies considered for the NLC are $\sqrt{s} = 350 \text{ GeV}$ (assuming that $m_t = 174 \text{ GeV}$ [14]) and $\sqrt{s} = 500 \text{ GeV}$.

3. Results and conclusions

For simplicity, the W^\pm boson entering in the final states (1)–(2) has been kept on-shell in our calculations. Furthermore, to allow for the detection of the four jets we have imposed that these are all sufficiently energetic and well separated, by imposing the cuts $E_j > 5$ GeV and $\cos\theta_{jj} < 0.95$, for all kind of jets $j = j, b$ in the final states (3)–(4). Finally, as reference values for the b -tagging efficiency ϵ_b and non- b rejection factor R_b we adopt the ‘conservative’ values 0.5 and 50, respectively [5, 6]. In carrying out the discussion presented in this Section we closely follow those of Refs. [1, 2], which are based on the top and Higgs detection strategies exposed in Refs. [10] and [11].

In detail, the selection procedures of top-antitop signals at the NLC usually considered are (see Ref. [12]): *i*) to perform a scan in \sqrt{s} ; *ii*) to study the W^\pm momentum spectrum; *iii*) to reconstruct the invariant mass of the three-jet system $t \rightarrow bW^\pm \rightarrow bj\bar{j}$. The first two methods are normally used at threshold ($\sqrt{s} \approx 2m_t$), whereas the last one has been considered for studies far above that ($\sqrt{s} \gg 2m_t$). Those for Higgs selection are in general: *i*) the ‘missing mass’ analysis (for two-body Higgs production); *ii*) the ‘direct reconstruction’ method (for all Higgs production mechanisms). They are both described in Ref. [13], and the procedure is always to reconstruct the Higgs resonance: in the first case via the spectrum in the recoil mass $M_{\text{recoil}}^2 = [(p_{e^+} + p_{e^-}) - (p_b + p_{\bar{b}})]^2$ (since $Z, A \rightarrow b\bar{b}$); in the second case directly from the Higgs decay products (in $\phi, H \rightarrow W^-W^+ \rightarrow W^\pm jj$).

In Fig. 2 we scan the energy range $2m_t - 10$ GeV $\lesssim \sqrt{s} \lesssim 2m_t + 10$ GeV by computing the cross sections for producing events of the type $W^\pm + bbj\bar{j}$ and $W^\pm + jjj\bar{j}$ via QCD. As stressed in Ref. [13], a cut in the minimum value of the hadronic mass $M_h \equiv M_{\text{jets}}$ is generally helpful in suppressing the reducible background, and we have implemented it here³ [12]. For a top mass of 174 GeV, we adopt the requirement $M_h > 200$ GeV [2]. From Fig. 2 one notices that the cross sections for the QCD processes (3)–(4) are rather large before the implementation of the M_h selection cut. In fact, one should remember that, for $\sqrt{s} \approx 2m_t$, the rates for top-antitop events are a few hundred femtobarns, and the ones for the irreducible EW background are of 10 fb or so, with cuts in energy and cosine not yet implemented (see Ref. [2]). The need for the hadronic mass constraint is then clear, if one notices that, e.g., for $\sqrt{s} = 350$ GeV, the cross sections after cuts for events of the type $W^\pm + bbj\bar{j}$ and $W^\pm + jjj\bar{j}$ are 0.16 and 22.40 fb, respectively, whereas the corresponding total rates were at the beginning (i.e., before cuts) 4.75 and 934.20 fb ! By considering that a further rejection factor $R_b^2 \approx 2500$ against light quark and gluon jets will multiply in the end the rates of $W^\pm + jjj\bar{j}$ events and that an overall efficiency to tag two b -quarks $\epsilon_b^2 \approx 0.25$ will multiply the irreducible background rates containing two b ’s, one should conclude that the total background in $W^\pm + 4\text{jet}$ events via QCD amounts to a few percent of the EW one, around the threshold at $\sqrt{s} = 350$ GeV (compare to the rates given in Refs. [1, 2]).

Fig. 3 shows the distribution in the momentum of the (tagged) W^\pm boson for events of the type (3)–(4). For reference, we also plot the same spectrum in case of top-antitop events decaying into $W^\pm + bbj\bar{j}$ (including finite Γ_t effects, see Refs. [1, 2]). The same cuts (in E_j , $\cos\theta_{jj}$ and M_h) have been applied to all processes (QCD background and $t\bar{t}$). Like in the case of integrated rates, no significant impact should be expected from QCD events in this case, being the main smearing effects due to finite top width and irreducible EW

³In contrast, note that such a constraint is not that effective in eliminating the irreducible EW background, see discussions in Ref. [1, 2].

background [1, 2].

At $\sqrt{s} = 350$ GeV the bremsstrahlung channel $e^+e^- \rightarrow Z\phi$ is the dominant \mathcal{SM} Higgs production mechanism, and (as stressed in Refs. [1, 2]) the channel $Z\phi \rightarrow (b\bar{b})(W^+W^-)$ might well be one of best ways to detect a heavy Higgs, thanks to the expected performances of the vertex detectors in triggering the Z boson [15]. Furthermore, the mode $Z \rightarrow b\bar{b}$ has a branching ratio (BR) about five times larger than that into $\mu^+\mu^-$ or e^+e^- and it is equally free from backgrounds coming from W^\pm decays. In Fig. 4a we plot the differential distribution in the invariant mass of all the possible $W^\pm jj$ combinations for the signatures (3)–(4), since the Higgs resonance will be searched for in the decay chain $\phi \rightarrow W^+W^- \rightarrow W^\pm jj$. For reference, in the same figure we have superimposed the rates for the Higgs signal (as an example, in the \mathcal{SM}). We assume a detector resolution of 10 GeV, such that the rates in Fig. 4a for the \mathcal{SM} Higgs process are nothing else than the total cross section for $e^+e^- \rightarrow Z\phi \rightarrow b\bar{b}W^+W^- \rightarrow bbW^\pm jj$ divided by ten (with the cuts in E_j and $\cos\theta_{jj}$ implemented). Since the Higgs and $W^\pm + bbjj$ rates in Fig. 4a must be multiplied by ϵ_b^2 whereas those for $W^\pm + jjjj$ must be divided by $R_{\bar{b}}^2$, it is clear that for \mathcal{SM} Higgs masses up to 250 GeV or so the number of background events should not modify the chances of Higgs detection. In fact, e.g., for $M_\phi = 160$ GeV, one gets (after b -tagging) 18 events for the \mathcal{SM} Higgs process and practically none from $W^\pm + bbjj$ and $W^\pm + jjjj$; whereas, for $M_\phi = 240$ GeV, the corresponding rates are 4.5 and 0.5 events (assuming $\int \mathcal{L}dt = 10 \text{ fb}^{-1}$ of integrated luminosity per annum). The same can be said also for the case of below threshold decays $\phi \rightarrow W^\pm W^{\mp*} \rightarrow W^\pm jj$, for Higgs masses $M_\phi \lesssim 160$ GeV, where the total number of signal events is indeed much larger than that of $W^\pm + 4\text{jet}$ events, by more than one order of magnitude⁴. For \mathcal{SM} Higgs masses larger than 250 GeV, the possibilities of Higgs detection appear to diminish significantly. On the one hand, phase space effects due to the limited collider energy available strongly suppress the Higgs production rates. On the other hand, both the $W^\pm + 4\text{jet}$ backgrounds become competitive with the signal⁵. Therefore, for $M_\phi \gtrsim 250$ GeV, not only would one need to exploit a higher luminosity option, but also would have less control on the backgrounds. For example (assuming now that $\int \mathcal{L}dt = 100 \text{ fb}^{-1}$), for a Higgs mass of 270 GeV, one gets the following number of events: 1.7 for the signal, and about 7 for the total $W^\pm + 4\text{jet}$ background.

In this context, however, one could always resort to a cut in the invariant mass of the $b\bar{b}$ pair, as for the signal the corresponding spectrum will peak at the Z mass, whereas for the background the di-jet mass distributions follow the behaviours displayed in Fig. 4b. A cut around M_Z , for example $|M_{jj} - M_Z| < 15$ GeV (as advocated in Ref. [13]), should be enough to remove the irreducible QCD backgrounds in $W^\pm + 4\text{jet}$ events.

For a higher energy NLC (i.e., $\sqrt{s} = 500$ GeV), irreducible background effects due to QCD events have no importance in top searches, as can be clearly seen from Fig. 5. After

⁴Note that in the range $140 \text{ GeV} \lesssim M_\phi \lesssim 2M_W$ the off-shell two-boson decay has a branching ratio comparable or even larger than that in $b\bar{b}$ pairs, making its exploitation important. In fact, in case of $\phi \rightarrow b\bar{b}$ decays one would have combinatorial problems, because of the presence of four b -quarks in the final state. Mistags are instead absent in the case of the $W^{\pm*}W^\mp$ channel (at least for high b -tagging performances).

⁵Indeed, it should also be noticed that for $M_\phi \gtrsim 250$ GeV one has that $\Gamma_\phi \gtrsim 4$ GeV, so that the Higgs width starts becoming similar to the invariant mass resolution and not all Higgs events are contained in a 10 GeV bin centered around the resonance. To increase the signal rates, one should consider additional bins. Inevitably, this procedure enhances the relative number of background events. This also means that the dotted curve slightly overestimates the rates for $M_\phi \gtrsim 250$ GeV. Note that similar comments will hold also at $\sqrt{s} = 500$ GeV, see Fig. 6a later on.

b -tagging suppression, the $W^\pm + 4\text{jet}$ rates are more than four orders of magnitude below the top-antitop ones (for mass resolution of 10 GeV or so), after the application of the constraint $0.95 \leq x_E \leq 1.05$, where $x_E = E_{bW \rightarrow 3\text{jets}}/E_{\text{beam}}$ [13].

In the case of Higgs searches at $\sqrt{s} = 500$, the prospects look even more promising than at lower energy. In fact, the number of $W^\pm + 4\text{jet}$ background events via QCD is always much smaller than that of the signal, for Higgs masses up to about 400 GeV (after b -tagging): that is, the kinematic border $\sqrt{s} - M_Z$ for Higgs production via the bremsstrahlung mechanism, see Fig. 6a. In addition, the usual cut in di-jet invariant mass to enhance the $Z \rightarrow b\bar{b}$ decay of the $Z\phi$ signal will reduce $W^\pm + 4\text{jet}$ rates to negligible levels (see Fig. 6b). In fact, the invariant masses produced by gluon splitting tend to concentrate towards low mass values (especially in $W^\pm + bbjj$ events, see graphs 1,2 & 4 in Fig. 1a), being instead the Higgs rates dictated by a 2.5 GeV wide Breit-Wigner distribution centered at M_Z .

In conclusion, effects due to irreducible background events via QCD interactions in processes of the type $e^+e^- \rightarrow W^\pm + bbjj$ and $e^+e^- \rightarrow W^\pm + jjjj$, which produce signatures similar to those of top and \mathcal{SM} heavy Higgs in the channels $e^+e^- \rightarrow t\bar{t} \rightarrow b\bar{b}W^+W^-$ and $e^+e^- \rightarrow Z\phi \rightarrow b\bar{b}W^+W^-$ (with $W^+W^- \rightarrow W^\pm jj$) at the NLC, are generally much smaller compared to those due to $e^+e^- \rightarrow b\bar{b}W^+W^-$ background events proceeding via EW interactions. This is largely due to the performances expected from the b -tagging devices in suppressing the QCD background in light quark and gluon jets and to the event selection procedures exploiting the resonant kinematics of the signal events. In fact, on the one hand, the $W^\pm + jjjj$ production cross section via QCD is much larger than that for $e^+e^- \rightarrow b\bar{b}W^+W^- \rightarrow W^\pm bbjj$ EW events, on the other hand, the detected cross section (i.e., after flavour tagging but before the kinematic selection) of $W^\pm + 4\text{jet}$ events can be smaller by only one order of magnitude respect to that of $t\bar{t}$ production, and bigger than that of $Z\phi$ production. However, in the very end, the only EW rates (as already computed in Refs. [1, 2]) should give reliable account of the effects due to the irreducible background in both top [1] and Higgs [2] searches, provided that suitable kinematic selection criteria of the signals are adopted. To our opinion, it was nonetheless important to assess the quantitative importance of QCD background events, because of the many and high precision measurements of both top and Higgs parameters foreseen at the linear colliders of the next generation. In particular, this has been done here with an exact calculation of the relevant tree-level matrix elements in perturbative QCD. (We do not expect in fact that soft QCD phenomena in the hadronisation processes could modify our main results.) Furthermore, as reference example, we have concentrated here on the case of the \mathcal{SM} Higgs boson [1] only: however, our arguments are also valid in the $MSSM$ [2]. Even in the case of more detailed studies of the (colour) structure of $b\bar{b}W^+W^- \rightarrow b\bar{b}\ell\nu_\ell jj$ events (with $\ell = e, \mu$), such as those carried out in Ref. [3], the effects due to the QCD irreducible background are negligible compared to those due to the EW one. Finally, we have assumed throughout the analysis a simplified b -tagging procedure, which did take into account neither the different probabilities in misidentifying, on the one hand, light quarks and gluons and, on the other hand, c -quarks, as bottom quarks, nor the consequent combinatorics entering in the effective tagging efficiency. Anyhow, more sophisticated and realistic algorithms will certainly not change the conclusions drawn from this study.

Acknowledgements

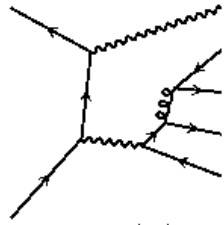
This work is supported in part by the Ministero dell' Università e della Ricerca Scientifica, the UK PPARC, and the EC Programme “Human Capital and Mobility”, Network “Physics at High Energy Colliders”, contract CHRX-CT93-0357 (DG 12 COMA).

References

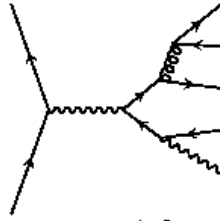
- [1] A. Ballestrero, E. Maina and S. Moretti, *Phys. Lett.* **B333** (1994) 434;
A. Ballestrero, E. Maina and S. Moretti, *Phys. Lett.* **B335** (1994) 460.
- [2] S. Moretti, *preprint Cavendish-HEP-96/3*, DFTT 19/96, March 1996 (to be published in *Z. Phys. C*).
- [3] V.A. Khoze, W.J. Stirling, S. Moretti, A. Ballestrero and E. Maina, *Z. Phys.* **C72** (1996) 71.
- [4] Proceedings of the Workshop “ e^+e^- Collisions at 500 GeV. The Physics Potential”, Munich, Annecy, Hamburg, 3–4 February 1991, ed. P.M. Zerwas, DESY 92–123A/B, August 1992, DESY 93–123C, December 1993.
- [5] CMS Technical Proposal, CERN/LHC/94-43 LHCC/P1, December 1994.
- [6] ATLAS Technical Proposal, CERN/LHC/94-43 LHCC/P2, December 1994.
- [7] T. Stelzer and W.F. Long, *Comp. Phys. Comm.* **81** (1994) 357.
- [8] H. Murayama, I. Watanabe and K. Hagiwara, HELAS: HELicity Amplitude Subroutines for Feynman Diagram Evaluations, *KEK Report* 91-11, January 1992.
- [9] G.P. Lepage, *Jour. Comp. Phys.* **27** (1978) 192.
- [10] Section ‘Top Quark Physics’, P. Igo-Kemenes and J.H. Kühn conveners, in Ref. [4] (and references therein), part A.
- [11] Section ‘Higgs Particles’, D. Haidt, R. Kleiss and P.M. Zerwas conveners, in Ref. [4] (and references therein), part A.
- [12] G. Bagliesi *et al.*, in Ref. [4], part A.
- [13] P. Grosse-Wiesmann, D. Haidt and H.J. Schreiber, in Ref. [4], part A.
- [14] A. Caner, Presented at “*Rencontres du Physique de la Valle d’Aoste*”, March 1996;
M. Narain, Presented at the ‘*Rencontres du Physique de la Valle d’Aoste*’, March 1996.
- [15] Proceedings of the Workshop on “*High Luminosities at LEP*”, CERN Report 91-02, Geneva, Switzerland.

Figure Captions

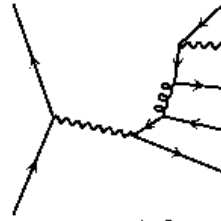
- [1] Relevant Feynman diagrams contributing at lowest order to processes (1) and (2): a) $W^\pm + q\bar{q}'Q\bar{Q}$ case; b) $W^\pm + q\bar{q}'GG$ case. Permutations of real and virtual lines along the fermion lines are not shown. An internal wavy line represents a W^\pm , a γ and a Z , as appropriate.
- [2] Cross section around the top-antitop threshold $2m_t \approx 350$ GeV for the final states (3) and (4). The underlying cuts $E_j > 5$ GeV and $\cos\theta_{jj} < 0.95$ have been implemented on all (gluon, light and heavy quark) jets in the final states. Upper curves are before cuts, lower curves are after the cut $M_h > 200$ GeV.
- [3] Differential distribution in the momentum of the W^\pm boson, for events of the type (3) and (4), at $\sqrt{s} = 350$ GeV. The underlying cuts $E_j > 5$ GeV and $\cos\theta_{jj} < 0.95$ have been implemented on all (gluon, light and heavy quark) jets in the final states. The top selection requirement $M_h > 200$ GeV has been also implemented. The shaded histogram represents the rates obtained from the process $e^+e^- \rightarrow t\bar{t} \rightarrow b\bar{b}W^+W^- \rightarrow W^\pm + bbjj$ (for $\Gamma_t \neq 0$, see Refs. [1, 2]), with $m_t = 174$ GeV, for the same choice of cuts in E_j , $\cos\theta_{jj}$ and M_h .
- [4] Differential distribution in the invariant mass of all the possible: a) $W^\pm + 2$ jet combinations, b) 2jet combinations, for events of the type (3) and (4), at $\sqrt{s} = 350$ GeV. The underlying cuts $E_j > 5$ GeV and $\cos\theta_{jj} < 0.95$ have been implemented on all (gluon, light and heavy quark) jets in the final states. Bins are 10 GeV wide. The dotted line in a) represents the corresponding spectra in the case of \mathcal{SM} Higgs events in the $Z\phi \rightarrow b\bar{b}W^+W^- \rightarrow bbW^\pm jj$ channel, assuming a 10 GeV resolution on M_ϕ (note the onset of the $H \rightarrow ZZ$ decay channel at $M_\phi \approx 2M_Z$).
- [5] Differential distribution in the invariant mass of all the possible 3jet combinations, for events of the type (3) and (4), at $\sqrt{s} = 500$ GeV. The underlying cuts $E_j > 5$ GeV and $\cos\theta_{jj} < 0.95$ have been implemented on all (gluon, light and heavy quark) jets in the final states. The top selection requirement $0.95 < x_E < 1.05$ has been also implemented. The shaded histograms represent the rates obtained from the process $e^+e^- \rightarrow t\bar{t} \rightarrow b\bar{b}W^+W^- \rightarrow W^\pm 4$ jets (for $\Gamma_t \neq 0$, see Refs. [1, 2]), with $m_t = 174$ GeV, for the same choice of cuts in E_j , $\cos\theta_{jj}$ and x_E . Black shadowing: ‘right’ $W^\pm b$ combination; dotted shadowing: ‘wrong’ $W^\pm b$ combination (see Refs. [1, 2]).
- [6] Same as Fig. 4, at $\sqrt{s} = 500$ GeV.



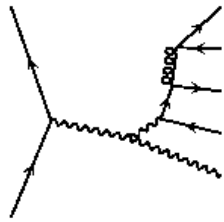
graph 1



graph 2

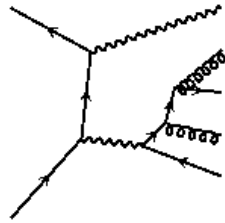


graph 3

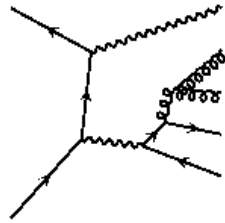


graph 4

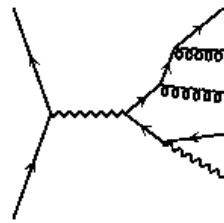
Fig. 1a



graph 1



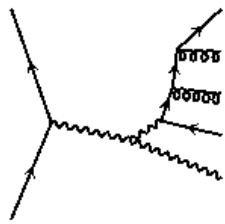
graph 2



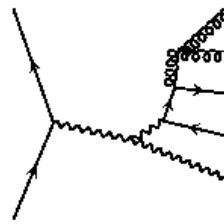
graph 3



graph 4



graph 5



graph 6

Fig. 1b

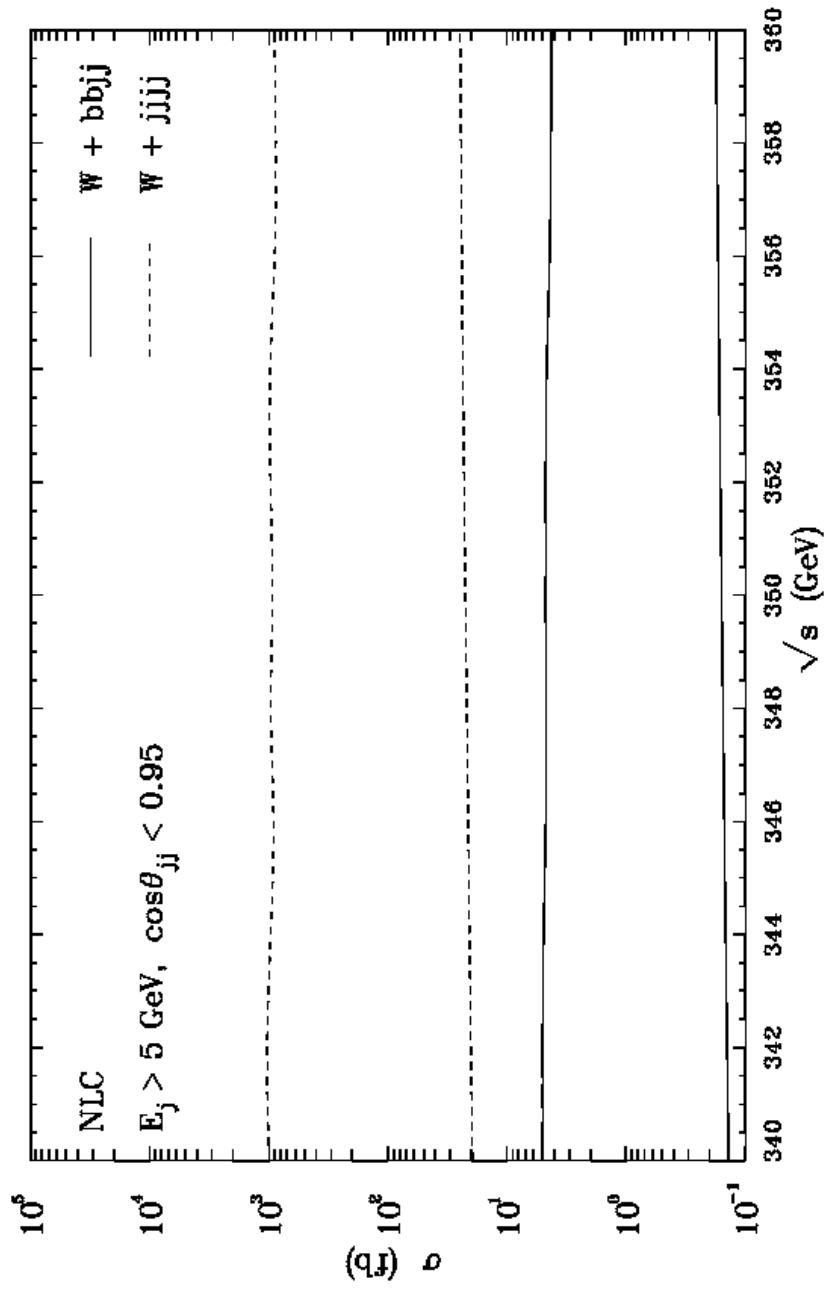


Fig. 2

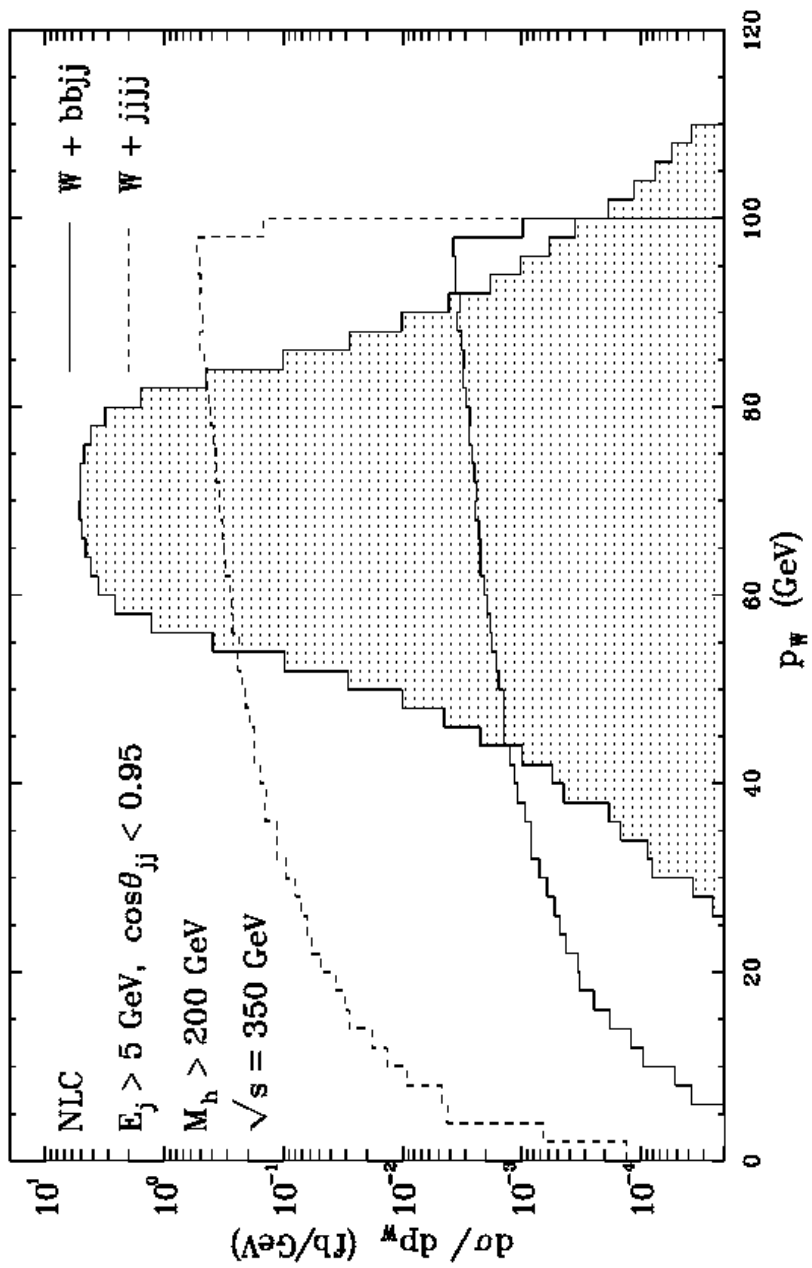


Fig. 3

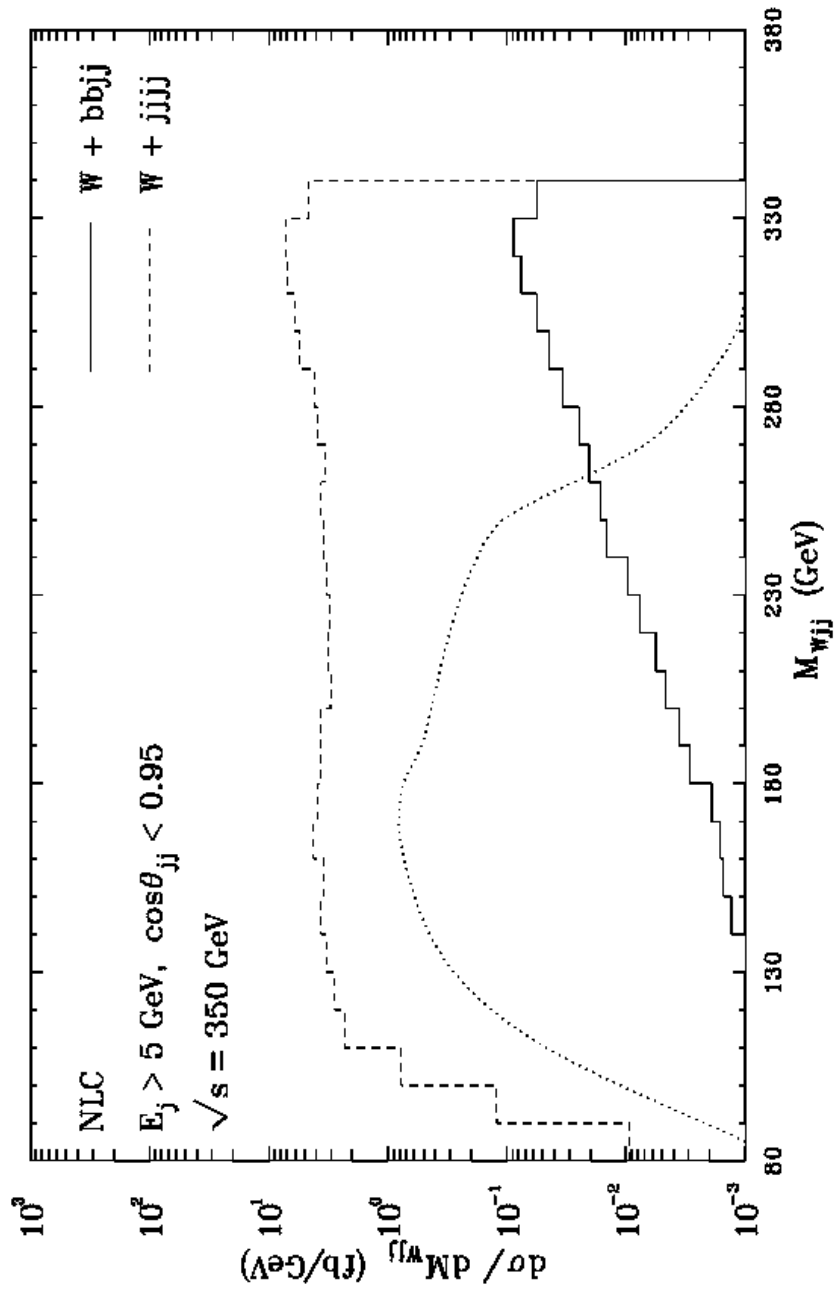


Fig. 4a

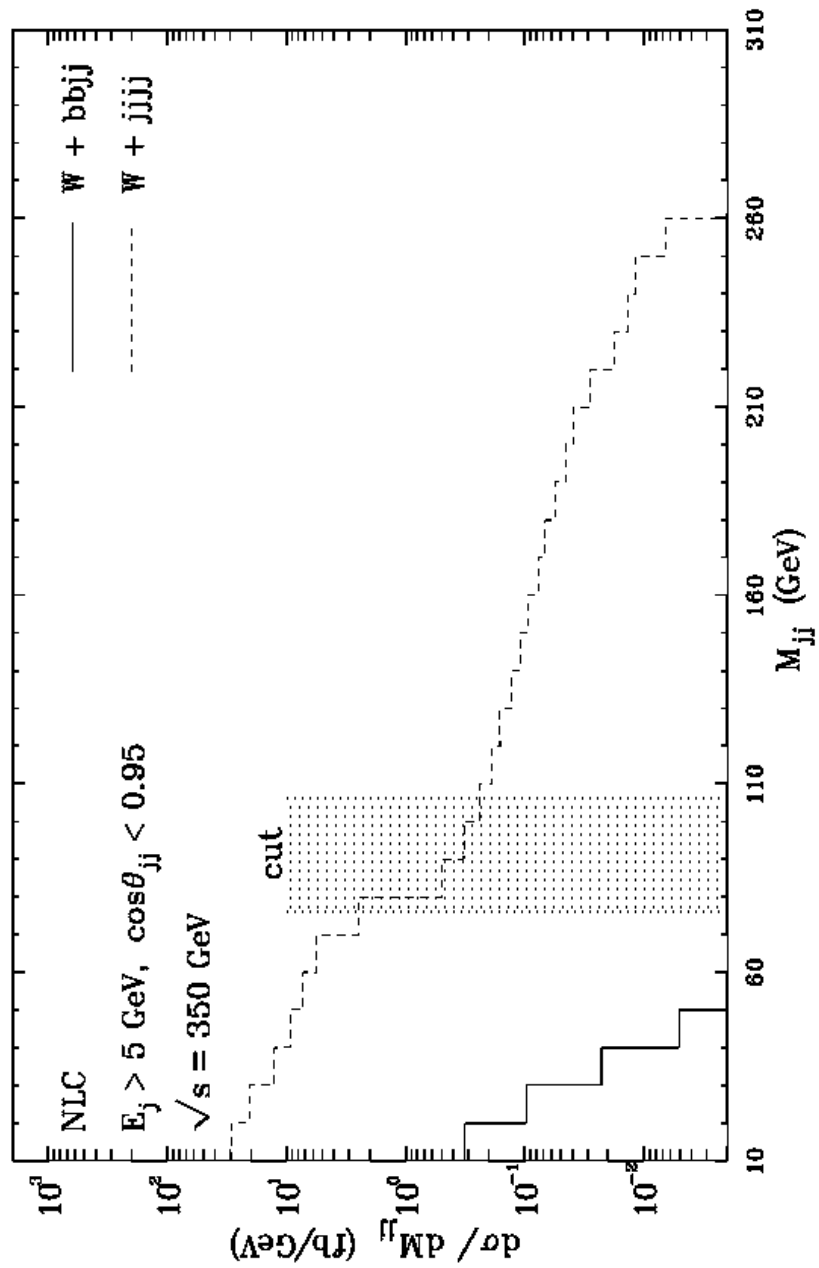


Fig. 4b

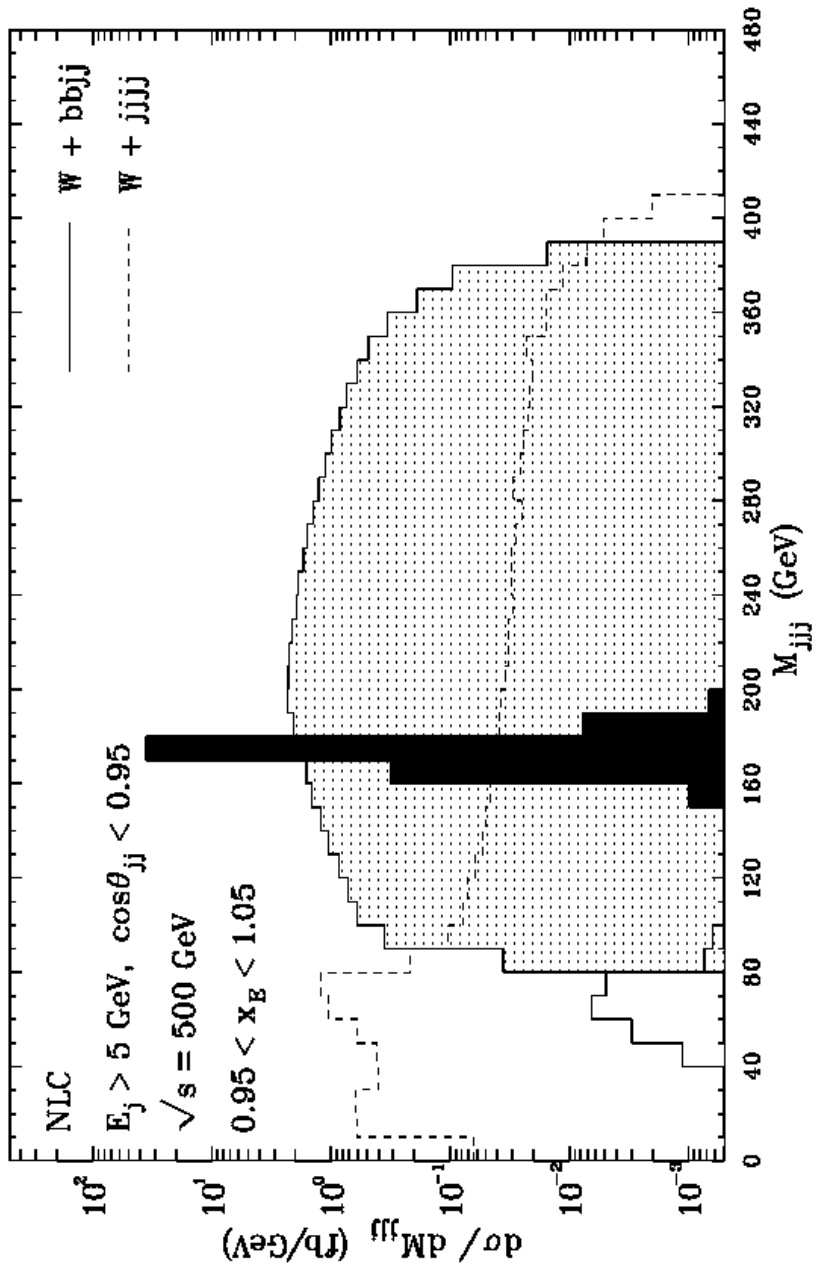


Fig. 5

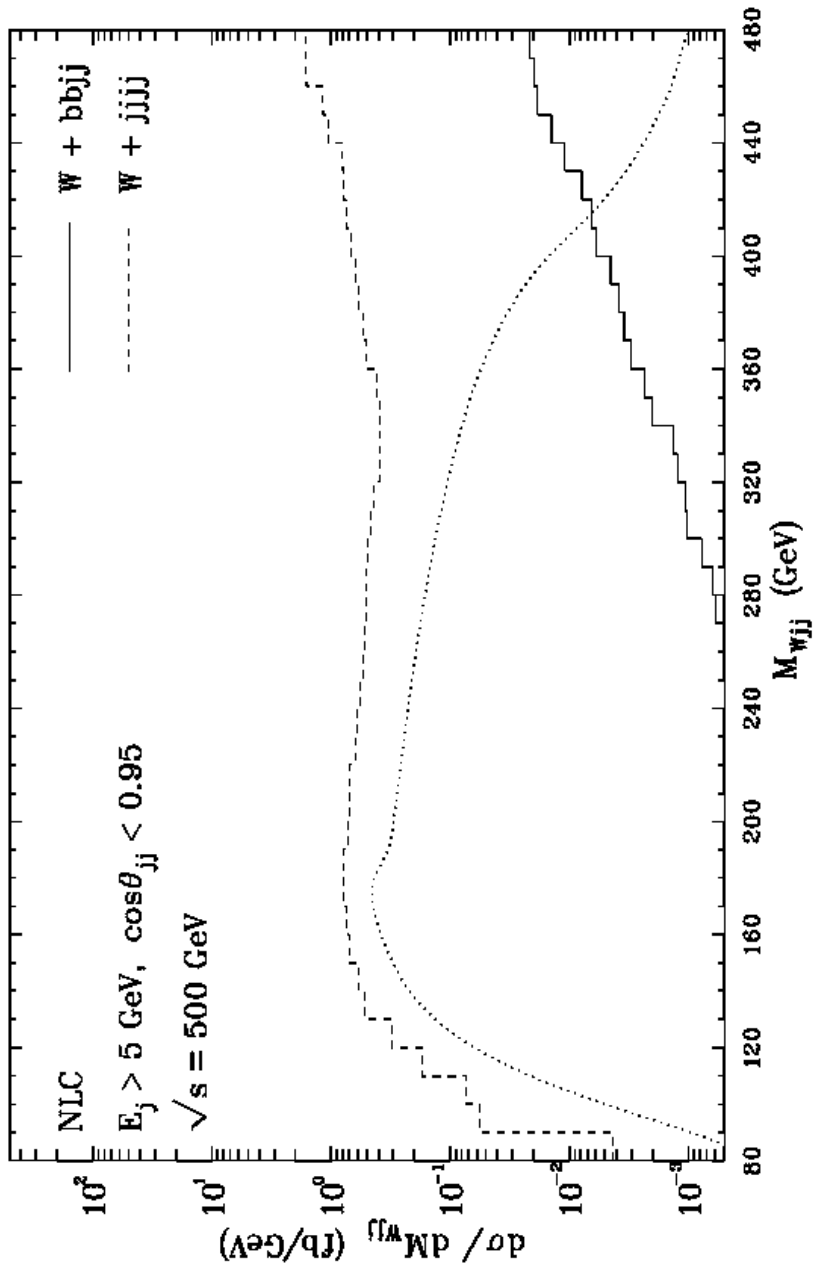


Fig. 6a

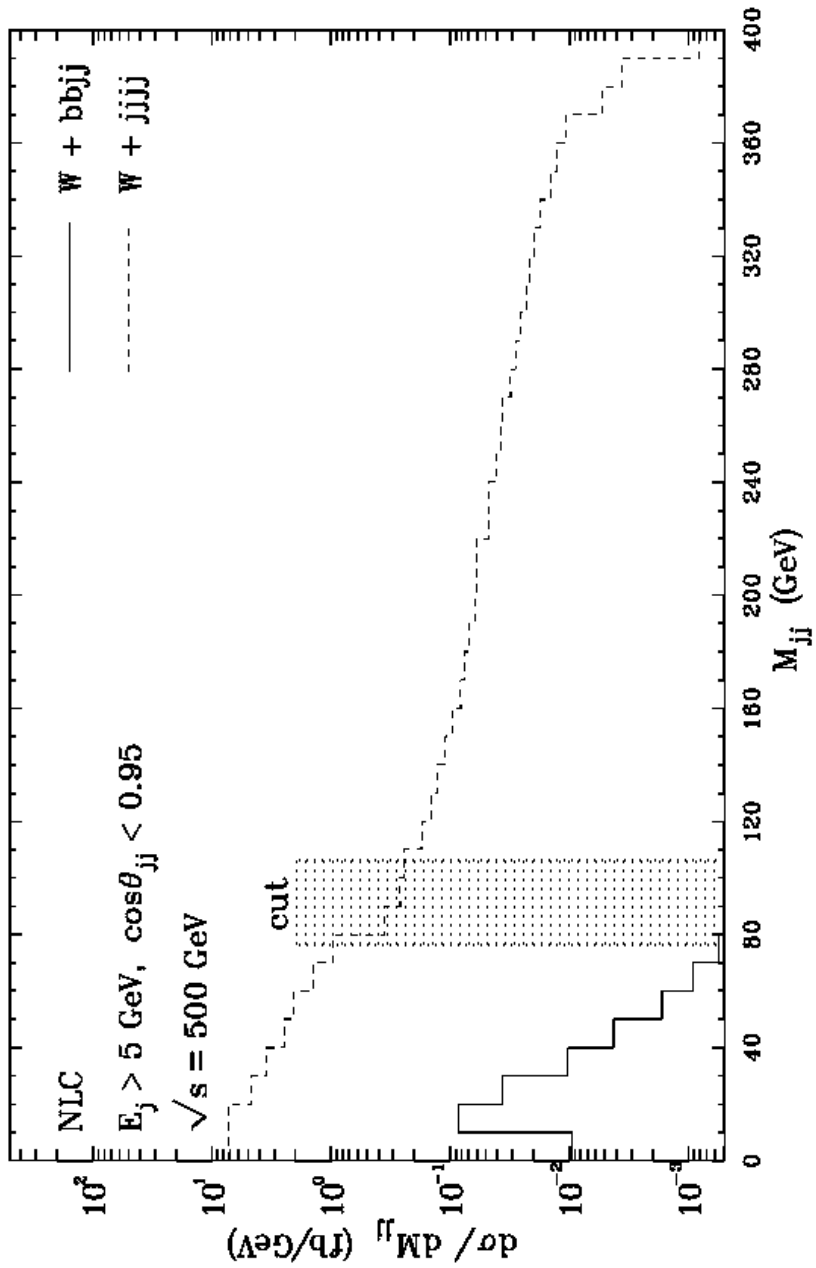


Fig. 6b